■ **PHYSICS SECTION**

# Annealing Dependence of Structural Characteristics of $Cu_2ZnSnS_4$ Films Deposited by Electrodeposition

A. E. Hassanien[1], H. Hashem[1], S. H. Moustafa[1], G. Kamel[1],

M. R. Balbol[2] and A. A. Ramadan[1]

[1]Physics Department, Faculty of Science, Helwan University, Cairo, Egypt
[2]National Researches Center For Radiation and Technology, Atomic Energy Authority, Cairo, Egypt

Semiconductors of I-II-IV-VI groups based on the kesterite structure ($A_2BCX_4$) as $Cu_2ZnSnS_4$ (CZTS) is an alternative compound for the absorber of solar cells. CZTS films contain naturally abundant and cheap Zn and Sn, i.e., they are free from the resource saving problem and the environmental pollution. Effect of annealing in different ambiences (air and sulfur) on the structural characteristics (formation of phases and their lattice parameters as well as crystallite size and distribution) of films prepared by electrodeposition was studied. X-ray spectroscopy and diffraction analyses were used to investigate the variation of the elemental analysis of the formed phase and their structure characteristics due to annealing and sulfurization. Raman spectroscopy was also used as a complementary investigation. Annealing of the as deposited films, especially in sulfur atmosphere, enhance the formation of CZTS phase and improve its crystallinity. Raman data is in good agreement with data obtained by XRD, in which CZTS phase obtained only after annealing process. The lattice dimensions of the as prepared samples are larger than that in JCPDS. The unit cell volume decreases by sulfurization. This is explained by the production of traces of one of the tin sulfide phases due to the presence of interstitial Sn as well as their thermodynamic stability. Sulfurization increases the width of relative distribution curve.

Keywords: CZTS films, XRD, lattice parameters, crystallitesize, sulfurization.

## 1. Introduction:

Thin film solar cells based on $CuInSe_2$ (CIS), $Cu2$ (In, Ga) $Se_2$ and $Cu_2$ (In, Ga) (S, Se)$_2$ (CIGS) have attracted considerable interest due to their high conversion efficiency; it reaches above ~ 22% for CIGS [1, 2]. Despite their promise for photovoltaic technologies with respect to reducing cost per watt of

solar energy conversion, each has some limitations: a) scarcity of In or Ga, and b) environmental issues (toxicity) associated with Se. It is desirable to consider material systems that employ less toxic and lower cost elements, while maintaining the advantages of the chalcopyrite materials. Quaternary $Cu_2ZnSnS_4$ (CZTS) based on the kesterite structure can be considered as an alternative compound due to: a) its direct band gap of $\approx 1.5$ eV [3], b) large absorption coefficient >104 cm-1[4], c) contains naturally abundant and cheap Zn and Sn instead of In and Ga and d) contains a less toxic S instead of Se.  CZTS thin films were prepared by vacuum techniques sputtering deposition [5], thermal evaporation [6] and pulsed laser deposition [7]. CZTS films are also prepared by non-vacuum techniques such as electrodeposition [8], spray pyrolysis [9], sol-gel [10] and Deposition of Nanocrystal based ink [11]. Non- vacuum techniques are favorable as they usually are economic, simple, fast and can be used also for large scale applications.

The work aims at investigation of the effect of annealing in different ambiences (air and sulfur) on the formed phases as well as the crystallographic characteristics of CZTS films. A simple non-vacuum techniques; electrodeposition, will be used. X-ray diffraction (XRD) analyses will be used to identify the phase formation and to study the variation of the lattice parameters as well as crystallite size and distribution, as crystallographic characteristics, due to annealing and sulfurization. Raman spectroscopy will be also used as a complementary investigation of the presentence of CZTS phase.

## 2. Experimental Work:

CZTS thin films were prepared by electrodeposition aseasy and cheap technique. Electrodeposited CZTS films were prepared from aqueous solution of 10 mM copper sulfate pentahydrate ($CuSO_4.5H_2O$), 30 mM zinc sulfate heptahydrate ($ZnSO_4.7H_2O$), 20 mM tin sulfate dehydrate ($SnSO_4.2H_2O$), 20 mM tartaric acid, 100 mM trisodium citrate and 10 mM sodium thiosulfate at room temperature.Electrodeposition was performed using three-electrode configuration with platinum as counter electrode, Ag/AgCl electrode as the reference electrode and fluorine doped tin oxide (FTO) coated glass substrate as the working electrode. Deposition runs under potentiostatic mode at step potential of -1.1 V for 10 min at room temperature without stirring.

The deposited CZTS films were thermal annealed in tube furnace in argon atmosphere at temperature of 500 ºC for 10 min with and without elemental
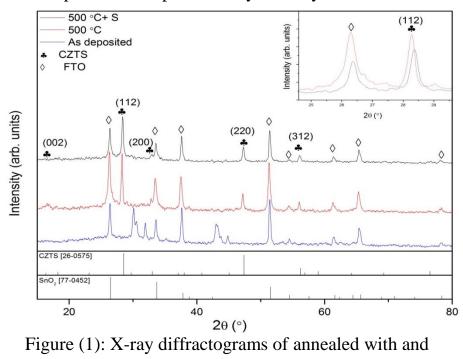
sulfur.For the purpose of comparison, two films of FTO were separately exposed to the same annealing conditions of temperature, time and atmosphere.

Structural analysis of the annealed CZTS were performed by X-ray diffractometer (Shimadzu XRD 6000) using Ni-filtered filtered CuKα radiation (λ = 1.54 Å) with 45 kV and 30 mA in the 2θ-range of 15 - 80º. Raman spectroscopy measurements were performed by "confocal Raman microscope" (WITec AlPHA 300 R) using laser excitation wavelength of 532 nm.

## 3. Results and Discussion:

### 3.1. Composition:

XRD diffractograms of the as-deposited films as well as those annealed with and without sulfur atmosphere are shown in Figs. (1). No XRD peaks corresponding toCZTS phase were observed for the as deposited films, Fig. (1), only those of the FTO substrate and other sulfide phases. Thus, some binary phases of Cu, Zn or Sn are likely to be formed depending on their lower energy of formation. Annealing with or without sulfur, enhances the formation of the CZTS phase.Using sulfur atmosphere, increase the relative peak intensities of CZTS phase to those of FTO. Annealing, especially in sulfur atmosphere, enhance the formation of CZTS phase and improve its crystallinity.



Figure (1): X-ray diffractograms of annealed with and without S-atmosphere (zoom in situ).

On annealing with and without sulfur atmosphere, beside the diffraction peaks of the FTO, peaks at 16.5, 28.3°, 32.8°, 47.2° and 56.04° are observed, which they attribute to the tetragonal kesterite structure (JCPDS Card no. 26-0575) of the planes (002), (112), (200), (220) and (312), respectively.

As a complementary phase investigation, Raman spectra of the electrodeposited films annealing with and without sulfur atmosphere are illustrated in Fig. (2). The spectra of the as deposited films did not show any evidence for the formation of CZTS phase in accordance with XRD results. However, as a result of annealing,evidence of phase formation where strong peak at 330 cm$^{-1}$ is observed that is the main characteristic peak of kesterite CZTS and close to the reported values [12, 13, 14]. Peaks located at250 cm$^{-1}$ and 289 cm$^{-1}$ and shoulder at 370 cm$^{-1}$ are reported to be from kesterite CZTS phase [15-17]. Small peak at 475 cm$^{-1}$ is attributed to copper sulfide phase [18], also peak at 428 cm$^{-1}$ is expected to be from copper sulfide phase as well. Peak at 192 cm$^{-1}$ may be related to tin oxide phase of the FTO substrate. The as deposited film show main weak peak at 270 cm$^{-1}$, which may related to tin sulfide $Sn_2S_3$. Raman data is in good agreement with data obtained by XRD, in which CZTS phase obtained only after annealing process.
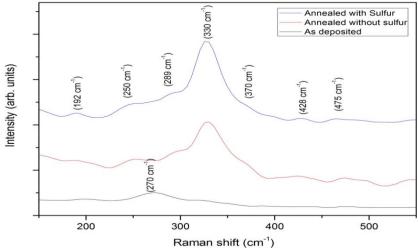


Figure (2): Raman spectra of annealed filmswith and without S-atmosphere.

## 3.2. Structural Characteristics:

The lattice parameters as well as the crystallite size and distribution are estimated from peak fitting and profile analysis using WINFIT program [19].Smoothing prior to fitting is considered redundant and may introduce

significant error into data [20]. Thus, a profile shape function is modeled to the experimental data and the interested characteristics are, then, calculated from the refined function (peak shape) parameters. Sample and standard peaks are fitted to Pearson VII profile function as illustrated in Fig. (3). The instrumental contribution is corrected by deconvolution using Stokes method implemented in the program. Crystallite size analysis was performed on single peak using integral breadth as well as Fourier analysisof Warren-Averbach [21] and the size distribution is obtained from the second derivative of the Fourier coefficients.

### 3.2.1.Lattice Parameters:

It was shown that the X-ray diffraction peaks of CZTS films on FTO or glass shift towards high 2θ-value after sulfurization. Also, the same shift was observed for the peaks of the bottom (lower) FTO film. This shift towards high diffraction angle reveals a decrease in the lattice parameters, i.e., shrinkage of the unit cell dimensions. On the other hand, no peak shift was observed in diffraction patterns of uncoated FTO as in case when it is covered by CZTS film. Thus, the shrinkage in the coated FTO is, therefore,a result of the induced compression stress by CZTS film on the underneath FTO one.

So, to investigate the effect of sulfurization, variation of the lattice parameters due to annealing in sulfur atmosphere has to be compared with the values of the annealed films without sulfur. First, the value of a-axis was calculated from (220) plane, $d_{220}$. Using this estimated a-value and the (112) plane, $d_{112}$, the c-axis was then calculated. Calculated values of lattice parameters and cell volume are given in Table (1)[19]. Both axes are decreased with sulfurization and consequently the cell volume.

Table (1): Lattice dimensions for films with and without sulfurization.

| Condition Sulfurization | Lattice parameters, (Å) | | Cell volume ($Å^3$) |
|---|---|---|---|
| | a-axis | c-axis | |
| No | 5.4421 | 10.9855 | 325.35 |
| Yes | 5.4317 | 10.9369 | 322.69 |

It was observed that the lattice dimensions of the as prepared samples are larger than that in JCPDS(26-0575): a = 5.427Å, c = 10.849Å and V = 319.50 $Å^3$or the literatures [22-24]. This increase in unit cell volume cannot be simply

explained by replacement of a cation by another since the difference in ionic size is small. However, the possible type of disorder (lattice defect) that results in an increase in cell dimensions is the interstitials of one of the small cations ($Cu^+$, $Zn^{+2}$ or $Sn^{+4}$).
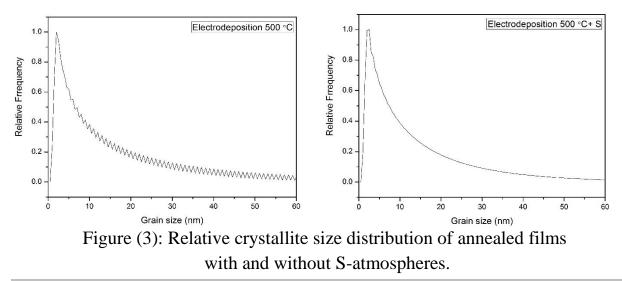
### 3.2.2. Crystallite Size:

Values of crystallite size estimated from XRD peak profile using two different analysis approaches are given in Table (2). In all cases, the sizes are within the nanoscale. On the other hand, values of crystallite sizes calculated by Fourier analysis (Warren and Averbach [21]), whichyields the mean coherently diffraction domains, are smaller than those calculated from integral breadth. This indicates that there are sub-grains and presence of twin and law-angle grain boundaries.

Table (4): Crystallite sizeof films annealed with and without sulfurization.

| Crystallite size (nm) | | |
|---|---|---|
| Sulfurization | Fourier analysis | Integral breadth |
| No | 2.02 | 4.6 |
| Yes | 1.57 | 3.16 |

The size of crystallite is greatly affect the electric properties of materials, however, not only the size but also its distribution is also important. Crystallite size distribution of the prepared CZTS films is illustrated in Fig. (3). Generally, no effect for the sulfurization on the width of distribution.



Figure (3): Relative crystallite size distribution of annealed films with and without S-atmospheres.

## 4. Conclusions:

- Annealing of the as deposited films, especially in sulfur atmosphere, enhance the formation of CZTS phase and improve its crystallinity.
- The unit cell volume decreases by sulfurization.
- Sulfurization increase the width of relative crystallite size distribution curve.
- The grain sizes are within the nanoscale and values of crystallite sizes calculated by Fourier analysis are smaller than those calculated from integral breadth.

### References:

(1) Tai, K.F., Kamada, R., Yagioka, T., Kato, T., Sugimoto, H., 2017. From 20.9 to 22.3% Cu (In,Ga)(S,Se)2 solar cell: reduced recombination rate at the heterojunction and the depletion region due to K-treatment. Jpn. J. Appl. Phys. **56** (8S2), 08MC03.

(2) Kamada, R., et al., 2016. New world record Cu(In,Ga)(Se,S)2 thin film solar cell efficiency beyond 22%. In: Photovoltaic Specialists Conference (PVSC), 2016 IEEE 43rd. IEEE, pp. 1287–1291.

(3) S.M. Pawar , A.I. Inamdar , K.V. Gurav , S.W. Shin , Yongcheol Jo , Jongmin Kim , Hyunsik Im , Jin Hyeok Kim , Vacuum **104**, 57-60 (2014).

(4) Hironori Katagiri, Kazuo Jimbo, Win Shwe Maw, Koichiro Oishi, Makoto Yamazaki, Hideaki Araki, Akiko Takeuchi, Thin Solid Films **517**, 2455–2460 (2009).

(5) Liu, Y.; Xu, J.; Yang, Y. and Xie, Z. (2016), *Superlattices and Microstructures*, **100**, 1283-1290.

(6) Sripan, C.; Madhavan, V. E.; Viswanath, A. K. and Ganesan, R. (2017), *Materials Letters*, **189**, 110-113.

(7)Pandiyan, R.; Elhmaidi, Z. O.;Sekkat, Z.; Abd-lefdil, M. and El- Khakani, M. A. (2017), Applied Surface Science, **396**, 1562-1570.

(8) Tao, J.; Chen, L.; Gao, H.; Zhang, C.; Liu, J.; Zhang, Y.; Huang, L.; Jiang, J.; Yang, P. and Chu, J., *Journal of Materials Chemistry A*, **4**, 3798 (2016).

(9) Prabeesh, P.; Saritha, P.; Selvam, I. P. and Potty, S. N., *Advanced Materials Proceedings*, **2**(1), 46 (2017).

(10) Guo, B. L.; Chen, Y. H.; Liu, X. J.; Liu, W. C. and Li, A. D., *AIP Advances*, **4**, 097115 (2014).

(11) Ghorpade, U. V.; Suryawanshi, M. P.; Shin, S. W.; Hong, C. W.; Kim, I.; Moon, J. H.; Kim, J. H.; and Kolekar, S. S., *Physical Chemistry Chemical Physics*, **17**, 19777 (2015).

(12) Seboui, Z; Cuminal, Y. and Kamoun-Turki, N., *Journal of Renewable and Sustainable Energy*, **5**, 023113 (2013).

13) Patro, B.; Vijaylakshmi, S.; Reddy, R. K. and Sharma, P., *Materials Today: Proceedings*, **3**, 2786 (2016).

14) Sakthivel, S. and Baskaran, V. *Nano Vision*, **5(7-9)**, 276 (2015),.

15) He, X.; Shen, H.; Wang, W.; Zhang, B.; Dai, Y. and Lu, Y., Journal of materials science: Materials in Electronics, 24, 572 (2013).

16) Wang, Y.; Ma, J.; Liu, P.; Chen, Y.; Li, R.; Gu, J.; Lu, J.; Yang, S.-E. and Gao, X., Materials Letters, 77, 13 (2012).

17) Sarswat, P. K.; Snure, M.; Free, M. L. and Tiwari, A., Thin Solid Films, **520**, 1694 (2012).

18) Shinde, N. M.; Lokhande, C.D.; Kim, J. H. and Moon, J. H., Journal of Photochemistry and Photobiology A: Chemistry, **235**, 14 (2012).

19) S. Krumm, An interactive Windows program for profile fitting and size/strain analysis, Mateials Science Forum, 228-231, 183-188 (1996).

20) Howard, S. A. andPreston, K. D., Prifile fitting of powder diffraction patterns, in Modern powder diffraction, Bich, D. L. and Post, J. E. (eds), Reviews in Mineralogy, **20**, 217-275 (1989).

21) Warren, B. E., Averbach, B. L., The effect of cold-work distortion on X-ray patterns, Journal of Applied Physics **21**, 595-599 (1950).

22) L. Burton and A. Walsh, J. Phys. Chem. C **116**, 24262 (2012).

23) Q. Guo, H. Hillhouse, and R. Agrawal, J. Am. Chem. Soc., **131**, 11672 (2009).

24) Chaochao Dun, N. A. W. Holzwarth, Yuan Li, Wenxiao Huang, and David L. Carroll, J. Appl. Phys. 115, 193513 (2014).